Research Letter DOI: 10.15541/jim20230428

Double Perovskite $Sr_2CoFeO_{5+\delta}$: Preparation and Performance as Cathode Material for Intermediate-temperature Solid Oxide Fuel Cells

CHEN Zhengpeng[1], JIN Fangjun[2,3], LI Mingfei[1], DONG Jiangbo[1], XU Renci[1], XU Hanzhao[4], XIONG Kai[5], RAO Muming[1], CHEN Chuangting[1], LI Xiaowei[2], LING Yihan[2]

(1. Guangdong Energy Group Science and Technology Research Institute Co., Ltd, Guangzhou 510000, China; 2. School of Materials Science and Physics, China University of Mining and Technology, Xuzhou 221116, China; 3. School of Physics, Changchun University of Science and Technology, Changchun 130022, China; 4. Guangdong Energy Group Co., Ltd., Guangzhou 510000, China; 5. Guangdong Huizhou LNG Power Co., Ltd., Huizhou 516000, China)

Abstract: Intermediate-temperature solid oxide fuel cells (IT-SOFCs), as the operating temperature decreases, require cathode materials with high catalytic activity. In this study, double perovskite $Sr_2CoFeO_{5+\delta}$ (SCF) was synthesized by Sol-Gel method, and effect of SCF cathode compounded with 20% (molar fraction) Sm_2O_3 doped CeO_2 (SDC) at different ratios on the electrode performance was elucidated. The SOFC single-cell performance was improved by optimized chemical expansion and area-specific resistance (ASR) from composite electrodes. Results show that, SCF cathode after annealing at 950 ℃ for 10 h exhibits good chemical compatibility with common electrolytes. For the composite of SCF and SDC at a mass ratio of 1∶1, the average thermal expansion coefficient (TEC) can be significantly reduced from 2.44×10^{-5} K^{-1} of pure SCF to 1.54×10^{-5} K^{-1}. ASR of SCF−*x*SDC (*x*=20, 30, 40, 50, *x*: mass percentage) composite cathodes are as low as 0.036, 0.034, 0.028 and 0.092 Ω·cm^2 at 800 ℃, respectively. The SCF−40SDC composite cathode displays the lowest ASR value among SCF−*x*SDC in the whole temperature range. Based on the 0.3 mm-thick $La_{0.9}Sr_{0.1}Ga_{0.8}Mg_{0.2}O_{3-\delta}$ (LSGM) electrolyte, the maximum power density of SOFC using SCF−40SDC (757 mW·cm^{-2}) as a cathode is higher than that of pure SCF (684 mW·cm^{-2}). These results demonstrate that the SCF−40SDC composite cathode is a promising candidate for application in IT-SOFCs.

Key words: solid oxide fuel cell; double perovskite; cathode; $Sr_2CoFeO_{5+\delta}$; composite electrode; electrochemical performance

Solid oxide fuel cell (SOFC) is one of the whole-solid-state chemical power generation devices that can directly convert the chemical energy stored in the fuel and oxidizer into electrical energy with high efficiency and low environmental impact. Traditional SOFCs operate at temperature as high as 1000 ℃, which causes material degradation and sealing problems, and greatly limits their commercialization. To overcome these disadvantages, researchers have sought to reduce the operating temperature of SOFCs[1-2]. For intermediate-temperature solid oxide fuel cells (IT-SOFCs), the reduction of operating temperature (500–800 ℃) imposes higher requirements on the catalytic performance of cathode materials. Perovskite-type oxides with certain oxygen ion conductivity become the focus of scientific research, as they maintain good electron conductivity with increasing ionic conductivity[2]. For example, Co-based perovskite cathodes $La_{1-x}Sr_xCo_{1-y}Fe_yO_{3-\delta}$[3-4] and $Ba_{0.5}Sr_{0.5}Co_{0.8}Fe_{0.2}O_{3-\delta}$[5-6] exhibit fast oxygen diffusion and high electrochemical performance as IT-SOFCs cathode materials. In particular, the most commercially successful cathode material, $La_{0.6}Sr_{0.4}Co_{0.2}Fe_{0.8}O_{3-\delta}$ (LSCF), shows excellent comprehensive properties (electrochemical performance and stability) at temperatures below 750 ℃. Recently,

Received date: 2023-09-20; **Revised date:** 2023-11-16; **Published online:** 2023-11-28
Foundation item: The Key-Area Research and Development Program of Guangdong Province (2022B0111130004); National Natural Science Foundation of China (52272257); Innovation Team of Jiangsu Province (JSSCTD202241)
Biography: CHEN Zhengpeng (1991–), male, Master. E-mail: chenzhengpeng@geg.com.cn
陈正鹏(1991–)，男，硕士. E-mail: chenzhengpeng@geg.com.cn
Corresponding author: LING Yihan, professor. E-mail: lyhyy@cumt.edu.cn; JIN Fangjun, associate professor. E-mail: jinfj@cumt.edu.cn
凌意瀚，教授. E-mail: lyhyy@cumt.edu.cn；金芳军，副教授. E-mail: jinfj@cumt.edu.cn

$LnBaCo_2O_{5+\delta}$-based (Ln=rare earth) oxides with a layer ordered double perovskite structure have been widely studied as IT-SOFCs cathode materials[7-11]. In this type of oxide, LnO and BaO layers are arranged along *c*-axis (⋯|CoO|BaO|CoO|LnO|⋯), and the oxygen vacancy is confined to the rare earth layer LnO. This specially ordered arrangement of ions forms a unique oxygen transport channel in the crystal, which is highly conducive to the transport of oxygen ions in the bulk phase.

Another type of double perovskite oxide, with the general formula $A_2B'B''O_{5+\delta}$, has been widely studied and has a strong application potential in the field of spintronics devices and information science[12-16]. Because A site is fully occupied by the low-valence alkaline earth metals, the material exhibits higher oxygen vacancy concentration. The ordered arrangement of B-site cations in the crystals also plays a key role in the electrochemical properties and charge/oxygen transport properties of the materials. It was found that the ionic conductivity of $Sr_2Fe_{1.5}Mo_{0.5}O_{6-\delta}$ (SFM) is 0.13 $S\cdot cm^{-1}$[17]. As a cathode material, ASR of SFM is 0.076 $\Omega\cdot cm^2$ at 800 ℃. Meng *et al*.[18] studied Ta^{5+} doped $Sr_2Fe_{1.5}Mo_{0.5-x}Ta_xO_{6-\delta}$ cathode material, showing that the substitution of Mo^{6+} by Ta^{5+} increases the oxygen vacancy concentration of the material and improves the ionic conductivity and electrochemical performance. Deng *et al*.[19] studied the B-ordered $Ba_2CoMo_{0.5}Nb_{0.5}O_{6-\delta}$ cathode material and found that the presence of Mo and Nb at the B-position stabilizes the Co ions in the mixed valence state. Due to high cost and chemical expansion from the traditional Co-based cathode materials, double perovskite oxide $Sr_2CoFeO_{5+\delta}$ (SCF) with various advantages of variable valence states of Co and Fe was proposed[12, 20-22]. In this study, based on the double perovskite SCF cathode material, the purpose of our consideration is to optimize the chemical expansion and catalysis activity to enhance the electrochemical performance of SOFC. SCF cathode was synthesized by Sol-Gel method, and systematic studies were conducted on its structural characterization, electrical conductivity, chemical compatibility, valence state, thermal expansion, and electrochemical performance of SCF samples. The properties of SCF−*x*SDC (SDC content: 20%−50% (in mass)) composite cathode materials were also assessed.

1 Experimental

Double-perovskite SCF oxide was synthesized by Sol-Gel method. Stoichiometric amounts of $Sr(NO_3)_2$, $Co(NO_3)_2\cdot 6H_2O$, and $Fe(NO_3)_3\cdot 9H_2O$ were weighed as start materials. The molar ratio of total metal ions: $(CH_2OH)_2$: $C_6H_8O_7$ was 1 : 2 : 2. The mixed solution became transparent under heating and stirring conditions. A homogeneous black viscous gel was obtained after evaporating the excess water. The gel was dried in the oven at 150 ℃ for 4 h, and the dried powders were subsequently calcined at 400 ℃ for 6 h and 900 ℃ for 10 h. The calcined powders were pressed into pellets by uniaxial molding at 220 MPa, and then sintered at 1200 ℃ for 10 h in the air to obtain the final composition with the desired SCF phase. $Ce_{0.8}Sm_{0.2}O_{1.9}$ (SDC), $Ce_{0.9}Gd_{0.1}O_{1.95}$ (GDC), and NiO powders were prepared by the glycine-nitrate process[23]. As for anode, NiO-SDC was prepared by finely mixing NiO and SDC at a weight ratio of 65 : 35. The composite cathodes were prepared by adding 20%–50% (in mass) SDC to pure SCF cathode, thoroughly grinding with an agate mortar for 2 h and denoted as SCF–20SDC, SCF–30SDC, SCF–40SDC, and SCF–50SDC, corresponding to SDC contents of 20%, 30%, 40%, 50%(in mass), respectively. Commercial La_2O_3, $SrCO_3$, Ga_2O_3, and MgO were used as raw materials for preparing $La_{0.9}Sr_{0.1}Ga_{0.8}Mg_{0.2}O_{3-\delta}$ (LSGM) electrolyte powder by the solid-state reaction method, and the dense LSGM electrolyte was obtained by sintering the samples at 1450 ℃ for 10 h. The preparation and packaging processes of single cell and symmetrical cells have been described elsewhere[9, 11].

Material characterization can be found in Supporting materials.

2 Results and discussion

2.1 Phase structure and chemical compatibility

Fig. 1(a) shows XRD pattern of SCF, and Rietveld refinement was performed with the GASA program, revealing that all reflections can be indexed to a cubic phase (space group $Fm\bar{3}m$)[12, 24-25]. The refined atomic parameters of SCF are given in Table S1, and the lattice parameter is a=0.7755(4) nm. The reasonable values of R factors (R_{wp}=6.75, R_p=3.81, and χ^2=1.37) confirm good refinement results. To test the chemical compatibility of SCF and electrolyte materials, SCF sample and common electrolytes (LSGM, CeO_2-based) were mixed at a weight ratio of 1 : 1. The mixed powder was calcined at 950 ℃ for 10 h, and the phase composition was analyzed by XRD test. Fig. 1(b) show XRD patterns of SCF−LSGM, SCF−SDC and SCF−GDC mixed powders after calcination at 950 ℃ for 10 h. The diffraction peaks of the mixed powder correspond to the physical superposition of the characteristic diffraction peaks of SCF and electrolytes, respectively. No new diffraction peaks or diffraction peak shifts were observed. Therefore,

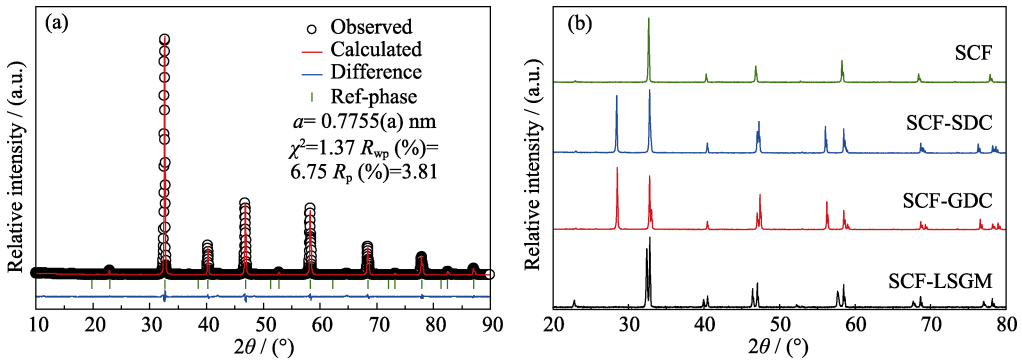

Fig. 1　XRD patterns of (a) Rietveld refined SCF and (b) mixture of SCF with different electrolyte materials

it is concluded that SCF samples have good chemical compatibility with LSGM, SDC and GDC electrolytes at 950 ℃.

2.2　Oxygen temperature programmed desorption

To investigate the transition metal reduction, the change of oxygen non-stoichiometric ratio and chemical stability of samples at high temperature, temperature-programmed desorption of oxygen tests were performed for SCF and SCF–40SDC(Fig. 2). The O_2-TPD curve of SCF exhibits three clearly distinguishable oxygen desorption peaks. Generally speaking, for perovskite oxides containing cobalt and iron, the α desorption peak of oxygen is attributed to the reduction of Co^{4+}/Fe^{4+} to Co^{3+}/Fe^{3+} at 300−600 ℃, and the β desorption peak of oxygen is attributed to the reduction of Co^{3+} to Co^{2+} above 700 ℃ [7, 26-27]. The formation process of α and β desorption peaks can be expressed by the defect equations (1) and (2).

$$2M_M^{\bullet}+O_O^{\times} \leftrightarrow 2M_M^{\times}+V_O^{\bullet\bullet}+\frac{1}{2}O_2 \quad (1)$$

$$2Co_{Co}^{\times}+O_O^{\times} \leftrightarrow 2Co'_{Co}+V_O^{\bullet\bullet}+\frac{1}{2}O_2 \quad (2)$$

Due to the high binding energy of Fe–O bond, it is believed that the peak near 450 ℃ is the oxygen α peak formed by the thermal reduction of Co^{4+} to Co^{3+} in SCF sample, and the peak near 580 ℃ is the oxygen α peak formed by the thermal reduction of Fe^{4+} to Fe^{3+} in SCF. With the increase of temperature, the thermal reduction of transition metals generates a large number of oxygen vacancies, which is conducive to further improving the oxygen transport and oxygen ion conductivity in the material. However, β peak of oxygen appeared near 720 ℃, contributing to further loss of oxygen in the sample. It is interesting that only α desorption peak of oxygen is detected in SCF−40SDC. The peak near 400 ℃ is the oxygen α peak formed by the thermal reduction of Co^{4+} to Co^{3+}, and the peak near 550 ℃ is the oxygen α peak formed by the reduction of Fe^{4+} to Fe^{3+}. Compared with pure SCF, SCF–40SDC shows no oxygen β-peak, which is due to the low-spin to high-spin transition of Co^{3+} ions in SCF with increasing temperature. The higher bond energy of the composite SDC has better interatomic bonding, which weakens the lattice expansion during the temperature rise, so further loss of lattice oxygen in the sample is prevented. In addition, Co and Fe in SCF−40SDC maintain high catalytic activity in +3 and +4 valence states at high temperature, which is conducive to improving the electrical and electrochemical activity of the material.

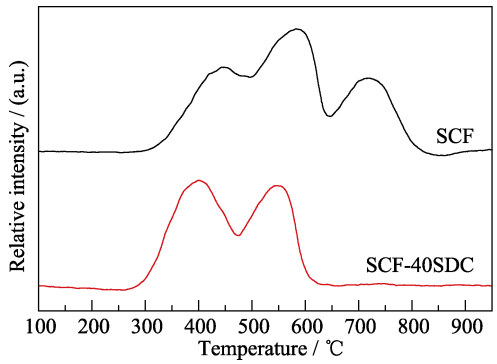

Fig. 2　O_2-TPD curves of SCF and SCF−40SDC

2.3　XPS analysis

Fig. 3(a) shows O1s XPS spectrum of the core level of SCF. The O1s peak with binding energy of 531.6 eV was derived from chemically adsorbed oxygen (O_{ads}), and the peak at 528.4 eV was derived from lattice oxygen (O_L) of the sample[28-29]. By calculating the relative intensity (peak area), the results show that O_L : O_{ads}=28 : 72 in the sample. The high levels of O_{ads} on the sample surface may be attributed to the presence of a large number of oxygen vacancies. This favors the adsorption/dissociation of oxygen ions both in the lattice and on the surface, which promotes ORR activity in the cathode material.

In Fig. 3(b), two characteristic positions of $Sr^{2+}3d_{5/2}$ and $3d_{3/2}$ in SCF are observed at 131.6 and 133.5 eV, respectively[30-31]. Satellite peaks at 132.0 and 135.2 eV may correspond to $Sr^{2+}3d_{5/2}$ and $3d_{3/2}$ in $SrCO_3$ of

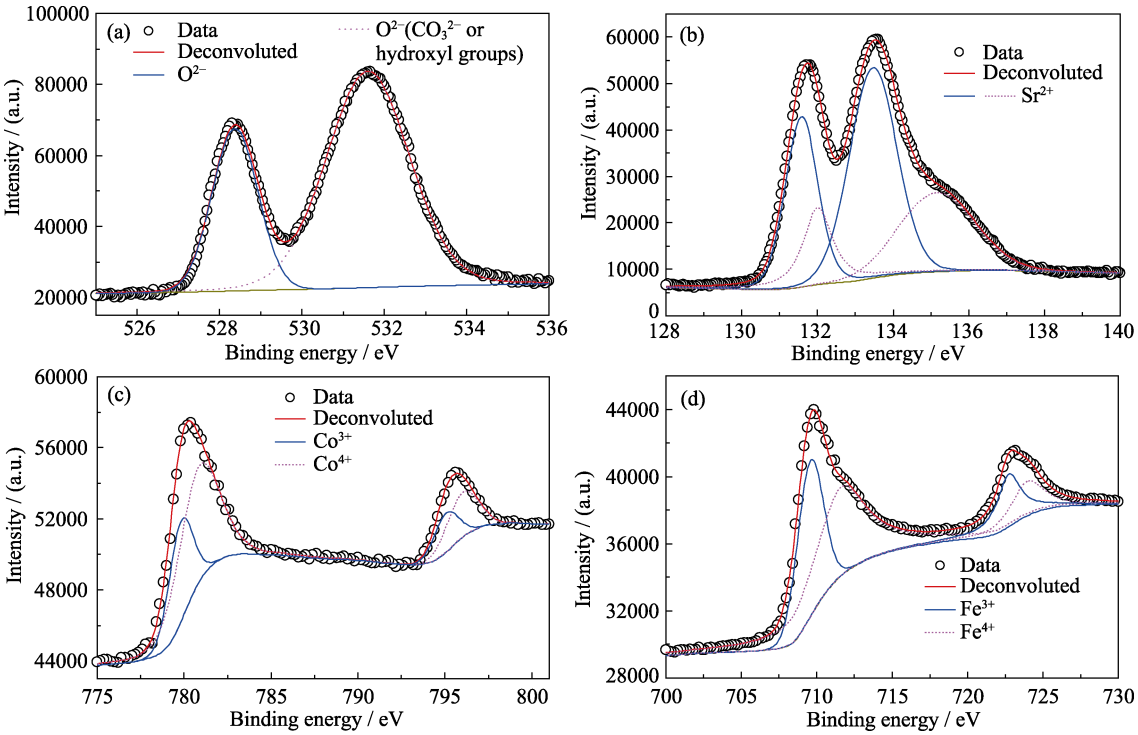

Fig. 3 Core-level XPS spectra of SCF at room temperature
(a) O1s; (b) Sr3d; (c) Co2p; (d) Fe2p

non-perovskite phase on the sample surface[30]. However, according to XRD results, the trace amount of carbonate had no effect on the material structure. As shown in Fig. 3(c), there are two pairs of different excited state spectral lines for Co2p$_{3/2}$ and 2p$_{1/2}$, respectively, indicating that there are two different valence states for Co ion in SCF. The peaks with binding energy of 779.5 and 794.2 eV belong to Co^{3+}2p$_{3/2}$ and 2p$_{1/2}$; the peaks with binding energy of 780.5 and 795.9 eV belong to Co^{4+}2p$_{3/2}$ and 2p$_{1/2}$[9, 11, 30]. In addition, the XPS spectrum of Co2p core level does not show the characteristic peak of Co^{2+} at (787.5±0.5) eV, so it can be concluded that the valence splitting in SCF samples is due to $Co^{3+/4+}$ mixed valence state without Co^{2+}[30]. As shown in Fig. 3(d), Fe2p XPS spectral lines can be divided into four peaks, among which the peaks with binding energies of 709.6 and 722.8 eV represent Fe^{3+}2p$_{3/2}$ and 2p$_{1/2}$, respectively. The peaks with binding energies of 711.6 and 724.0 eV represent Fe^{4+}2p$_{3/2}$ and 2p$_{1/2}$, respectively[8, 10, 29]. The result indicates that Co and Fe ions exist as +4 and +3 in SCF, as demonstrated by the O_2-TPD data. The results show that the proportion of Co^{4+} and Fe^{4+} is slightly higher than that of Co^{3+} and Fe^{3+}. According to the principle of electroneutrality, there are oxygen defects in SCF. The mixed valence Fe^{3+}/Fe^{4+} and Co^{3+}/Co^{4+} randomly occupy B' and B'' sites of the crystal space of SCF, respectively. According to XPS results, the oxygen content in the SCF sample was quantitatively calculated to be 5.62 (5+δ).

2.4 Thermal expansion analysis

Fig. 4 show (a) thermal expansion behaviors and (b) thermal coefficient differential curves of samples in the temperature range of 30−950 ℃. As shown in Fig. 4(b), a sudden change of thermal expansion can be observed near 400 ℃ for SCF, which is different from that of SCF−xSDC composite material (near 270 ℃). The sudden increase of the thermal expansion coefficient of SCF and its composites is closely related to the release of lattice oxygen and the formation of oxygen vacancy caused by the thermal reduction of Fe and Co ions in samples. This process corresponds to the oxygen α desorption peak of O_2-TPD in Fig. 2. As for composite SDC samples, the oxygen α desorption peak attributes to a shift towards lower temperatures, which corresponds to desorption of chemisorbed oxygen in the low-temperature range. Table 1 shows TEC of SCF−xSDC composite cathode materials in different temperature ranges. The introduction of SDC electrolyte significantly reduces the average TEC of the material. For example, the average TEC of SCF−50SDC at 30−300 and 300−950 ℃ is 12.5×10^{-6} and 16.3×10^{-6} K^{-1}, which are much lower than those of SCF. This is mainly due to the low TEC of SDC electrolyte (~12.3×10^{-6} K^{-1})[32]. Similar results are found for Pr/NdBaCoFeO$_{5+\delta}$−xSDC, NdBaCo$_{2/3}$Fe$_{2/3}$Cu$_{2/3}$O$_{5+\delta}$−xSDC and LaSrCoTiO$_{5+\delta}$−xSDC[29-30,33]. Compared with the single-phase SCF cathode, the chemical expansion coefficient of the composite cathode is smaller, which is also one of the reasons for low TEC of the composite cathode. The introduction of SDC

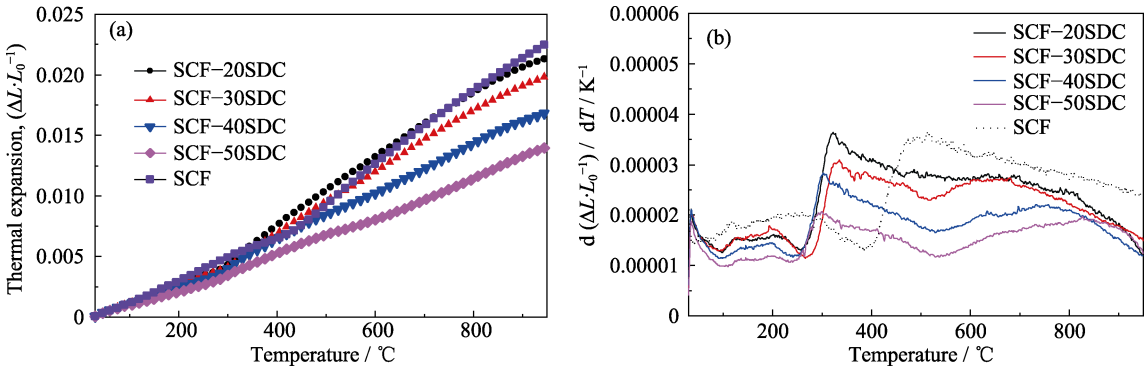

Fig. 4　(a) Thermal expansion behaviors and (b) thermal expansion coefficient curves of SCF–*x*SDC composite cathodes in the temperature range of 30–950 ℃

Colorful figures are available on website

Table 1 TEC of SCF–*x*SDC composite cathodes

Sample	Average TEC/($\times10^{-6}$, K^{-1})	
SCF	17.4 (30−400 ℃)	28.8 (400−1000 ℃)
SCF−20SDC	15.6 (30−300 ℃)	26.3 (300−950 ℃)
SCF−30SDC	15.0 (30−300 ℃)	24.3 (300−950 ℃)
SCF−40SDC	14.5 (30−300 ℃)	19.8 (300−950 ℃)
SCF−50SDC	12.5 (30−300 ℃)	16.3 (300−950 ℃)

electrolyte can not only reduce the TEC of materials, but also increase the oxygen ion conductivity, and improve the chemical stability and electrochemical performance of materials.

2.5　Conductivity

Fig. 5(a, b) show the conductivity and Arrhenius curves of SCF, respectively. The conductivity firstly increases, and then decreases with the increase of temperature, reaching the maximum at 350 ℃. Similar conductive behavior were reported in other cathode materials[8, 10, 24]. The maximum conductivity of SCF sample is 321 $S\cdot cm^{-1}$, which is not only higher than those of other double perovskite cathodes, such as P/NBCF[10] and $BaSc_{0.25}Co_{0.75}O_{3-\delta}$[34], but also comparable to that of the widely used $La_{0.6}Sr_{0.4}Co_{0.2}Fe_{0.8}O_{3-\delta}$ (LSCF) cathode[35]. The activation energy of the sample was calculated from the Arrhenius plot. In the low-temperature region, the activation energy of p-type Co^{3+}/Fe^{3+}−O−Co^{4+}/Fe^{4+} polaron of SCF is 8.3 $kJ\cdot mol^{-1}$, lower than those of Pr/$NdBaCo_{2/3}Fe_{2/3}Cu_{2/3}O_{5+\delta}$ (13.2 and 16.0 $kJ\cdot mol^{-1}$)[8, 29], which is beneficial for the redox reaction of cathode materials.

2.6　Electrochemical impedance

Fig. 6(a-d) show the typical impedance spectra of SCF−*x*SDC composite cathodes on the LSGM electrolyte in the temperature range of 700−800 ℃, Fig. 7(a, b) shows ASR and fitting lines of SCF−*x*SDC composite cathodes in the temperature range of 600−800 ℃. ASR depends significantly on the relative mass ratio of SDC and SCF. ASR of SCF−*x*SDC composite cathode firstly decreases, and then increases with the increase of SDC content. At 800 ℃, ASR of SCF−*x*SDC are 0.036, 0.034, 0.028, and 0.092 $\Omega\cdot cm^2$, respectively. ASR of SCF−40SDC composite cathode on LSGM electrolyte is the lowest, greatly improved the electrocatalytic activity of the material. These results suggest that the moderate introduction of ionic conducting SDC electrolyte into the SCF cathode material possesses different effects to decrease ASR. 1) Generally improve the oxygen diffusion rates and charge transfer of oxygen ions at the

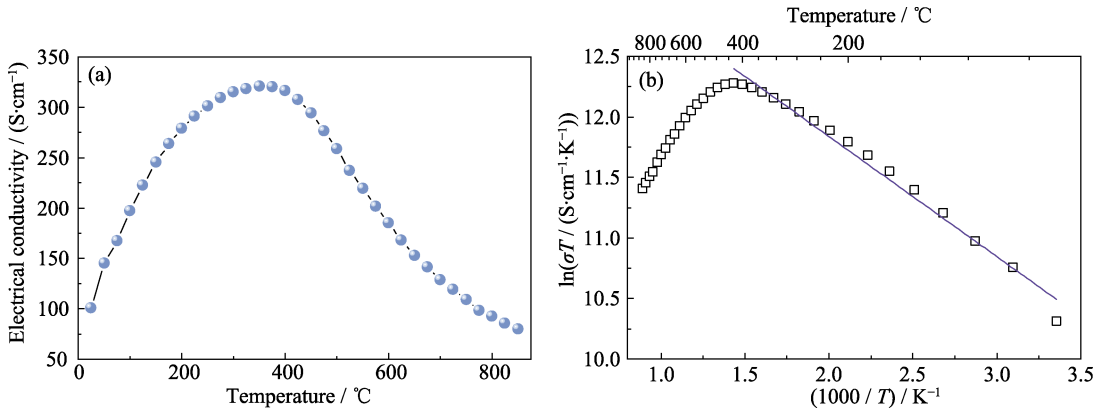

Fig. 5　(a) Temperature dependence of electrical conductivity and (b) Arrhenius plot of SCF

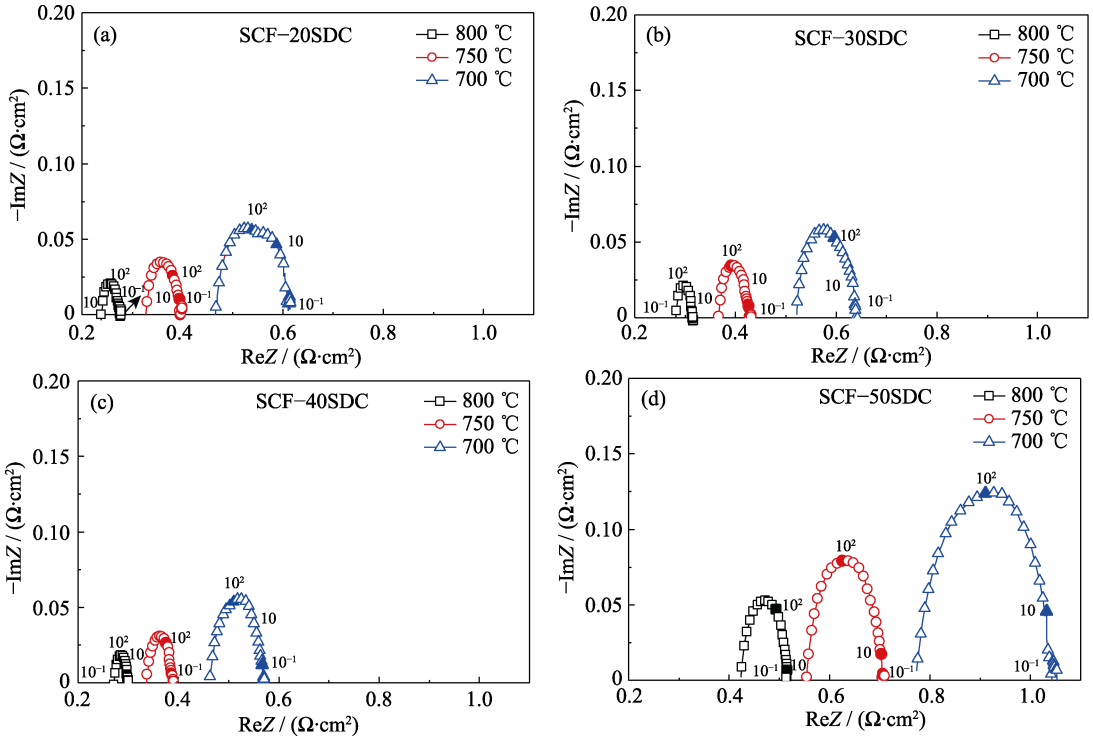

Fig. 6 Typical impedance spectra of SCF−*x*SDC composite cathodes

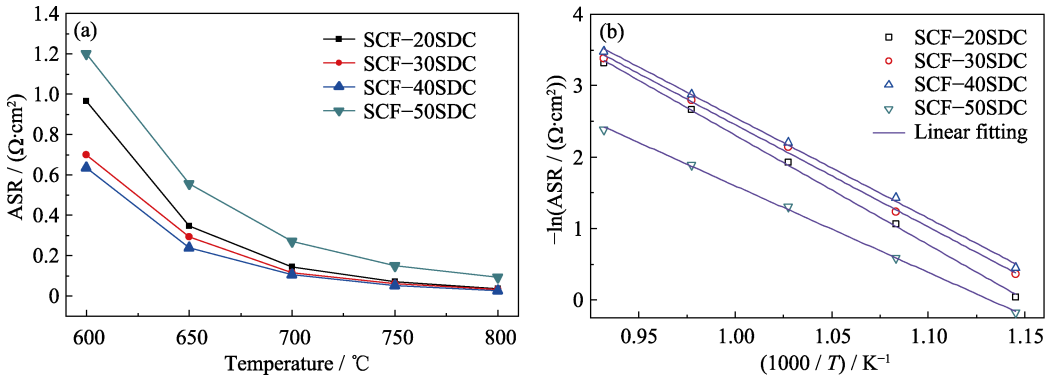

Fig. 7 (a) ASR and (b) Arrhenius plots of the polarization resistance for SCF–*x*SDC composite cathodes

electrolyte/electrode interface. 2) Homogeneously disperse on the SCF particles surface to form three-dimensional network of SCF and SDC phases in SCF–40SDC composite (Fig. S4), which increase the oxygen dissociation, diffusion, and transport processes[35]. 3) Improve the adhesion between cathode and electrolyte, enhances O^{2-} permeability from cathode to electrolyte. However, ASR increase as the SDC content rises above 40%(in mass) due to the significant reduction of TPB area and the increase in the network interruptions (including cathode and electrolyte), similar to other composite cathodes[30, 33, 36]. According to Arrhenius plots of ASR for SCF−*x*SDC composite cathodes, activation energies of SCF−*x*SDC composite cathode on LSGM electrolyte were calculated to be 127.5, 118.9, 117.3, and 100.6 kJ·mol^{-1}, respectively. Although SCF−50SDC composite cathode exhibits the smallest activation energy, its great ASR is not conducive to practical application. At 700 ℃, ASR of optimized SCF−40SDC composite cathode is 0.105 Ω·cm^2, significantly lower than the target value of 0.15 Ω·cm^2[37]. Therefore, SCF−40SDC composite cathode can be used as potential IT-SOFC cathode material.

2.7 Single cell performance

Fig. 8(a, b) show the *I–V* and *I–P* curves of the 0.3 mm electrolyte-supported Ni−SDC/SDC/LSGM/cathode using dry H_2 as fuel and ambient air as oxidant. The open circuit voltage is quite close to the expected Nernst potential, demonstrating that the cells were well sealed with dense LSGM electrolytes. The maximum power density increases monotonically with increasing temperature, which can be attributed to the decrease in resistance of the cell. As shown in Fig. 8, the maximum power densities of the cells are 684 and 757 mW·cm^{-2} for SCF and SCF−40SDC at 800 ℃, indicating better

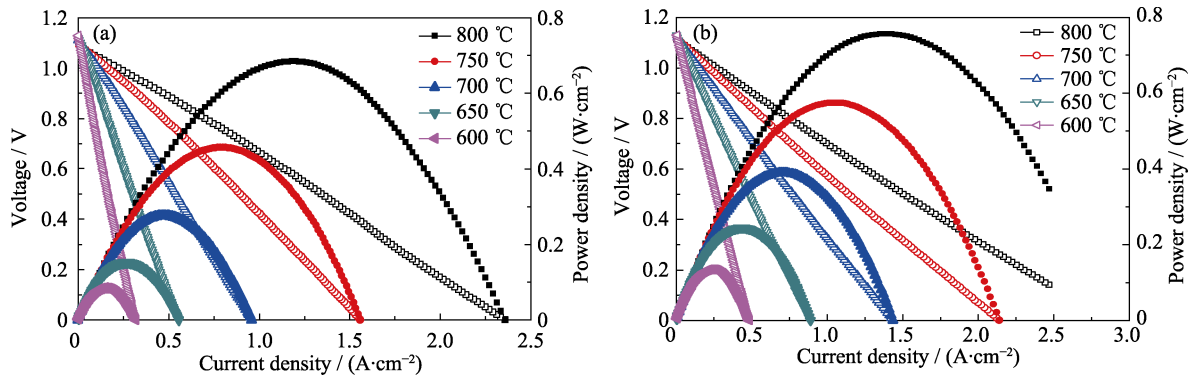

Fig. 8　*I–V* and *I–P* curves for (a) Ni−SDC|SDC|LSGM|SCF and (b) Ni−SDC|SDC|LSGM|SCF−40SDC at different temperatures

electrochemical activity of SCF−40SDC than pure SCF cathode. Compared with recent reported cathode materials (Table S2), SCF−40SDC obtained in this work displayed superior power density for its low TEC, excellent electrochemical performance and good chemical stability.

3　Conclusions

In this study, double perovskite SCF was successfully prepared by Sol-Gel method, and the SDC composite electrodes were mixed with different ratios in order to optimize the electrochemical properties of the SCF cathode. The XRD patterns show that SCF has good chemical compatibility with common electrolytes at 950 ℃ for 10 h, which is convenient for constructing composite electrodes. The decreased TEC can be observed from the SCF–*x*SDC composite cathode materials, and the average TEC were 2.44×10^{-5} and 1.54×10^{-5} K^{-1} for SCF and SCF−50SDC, respectively. TEC for the composite cathode close to the common electrolyte (SDC: 1.23×10^{-5} K^{-1}) shows that the cathode interfacial contact can be efficiently optimized during the intermediate-temperature operation, which facilitates diffusive oxygen transport on the cathode side. In addition, the SCF−40SDC composite cathode exhibited the lowest ASR value in all temperature ranges, indicating its higher electrocatalytic activity. The maximum power density of SOFC using SCF−40SDC (757 $mW\cdot cm^{-2}$) is higher than that of pure SCF (684 $mW\cdot cm^{-2}$) at 800 ℃, which exceeds most as-reported cathode materials. These results demonstrate that SCF−40SDC composite cathode is a promising candidate as cathode for application in IT-SOFCs.

Supporting materials

Supporting materials related to this article can be found at https://doi.org/10.15541/jim20230428

References:

[1] GUO T M, DONG J B, CHEN Z P, *et al*. Enhanced compatibility and activity of high-entropy double perovskite cathode material for IT-SOFC. *Journal of Inorganic Materials*, 2023, **38(6):** 693.

[2] HAN X, LING Y H, YANG Y, *et al*. Utilizing high entropy effects for developing chromium-tolerance cobalt-free cathode for solid oxide fuel cells. *Advanced Functional Materials*, 2023, **33(43):** 202304728.

[3] TAI L W, NASRALLAH M M, ANDERSON H U, *et al*. Structure and electrical properties of $La_{1-x}Sr_xCo_{1-y}Fe_yO_3$. Part 1. The system $La_{0.8}Sr_{0.2}Co_{1-y}Fe_yO_3$. *Solid State Ionics*, 1995, **76(3/4):** 259.

[4] TAI L W, NASRALLAH M M, ANDERSON H U, *et al*. Structure and electrical properties of $La_{1-x}Sr_xCo_{1-y}Fe_yO_3$. Part 2. The system $La_{1-x}Sr_xCo_{0.2}Fe_{0.8}O_3$. *Solid State Ionics*, 1995, **76(3/4):** 273.

[5] SHAO Z, HAILE S M. A high-performance cathode for the next generation of solid-oxide fuel cells. *Nature*, 2004, **431(7005):** 170.

[6] WEI B, LU Z, LI S Y, *et al*. Thermal and electrical properties of new cathode material $Ba_{0.5}Sr_{0.5}Co_{0.8}Fe_{0.2}O_{3-\delta}$ for solid oxide fuel cells. *Electrochemical and Solid State Letters*, 2005, **8(8):** A428.

[7] ZHANG K, GE L, RAN R, *et al*. Synthesis, characterization and evaluation of cation-ordered $LnBaCo_2O_{5+\delta}$ as materials of oxygen permeation membranes and cathodes of SOFCs. *Acta Materialia*, 2008, **56(17):** 4876.

[8] JIN F J, SHEN Y, WANG R, *et al*. Double-perovskite $PrBaCo_{2/3}Fe_{2/3}Cu_{2/3}O_{5+\delta}$ as cathode material for intermediate-temperature solid-oxide fuel cells. *Journal of Power Sources*, 2013, **234:** 244.

[9] LI J, SUN N, LIU X, *et al*. Investigation on $Nd_{1-x}Ca_xBaCo_2O_{5+\delta}$ double perovskite as new oxygen electrode materials for reversible solid oxide cells. *Journal of Alloys and Compounds*, 2022, **913:** 165245.

[10] JIN F, XU H, LONG W, *et al*. Characterization and evaluation of double perovskites $LnBaCoFeO_{5+\delta}$ (Ln=Pr and Nd) as intermediate-temperature solid oxide fuel cell cathodes. *Journal of Power Sources*, 2013, **243:** 10.

[11] LIU X, JIN F, SUN N, *et al*. Nd^{3+}-deficiency double perovskite $Nd_{1-x}BaCo_2O_{5+s}$ and performance optimization as cathode materials for intermediate-temperature solid oxide fuel cells. *Ceramics International*, 2021, **47(23):** 33886.

[12] BEZDICKA P, FOURNES L, WATTIAUX A, *et al*. Mössbauer characteristics of the Sr_2CoFeO_6 perovskite obtained by electrochemical oxidation. *Solid State Communications*, 1994, **91(7):** 501.

[13] MARTÍNEZ-LOPE MARÍA J, ALONSO JOSÉ A, CASAIS MARÍA T, *et al*. Preparation, crystal and magnetic structure of the double perovskites Ba_2CoBO_6 (B=Mo, W). *European Journal of Inorganic Chemistry*, 2002, **2002(9):** 2463.

[14] YOSHII K. Magnetic transition in the perovskite $Ba_2CoNbO_{6-\delta}$ *Journal of Solid State Chemistry*, 2000, **151(2):** 294.

[15] COX D E, SHIRANE G, FRAZER B C. Neutron-diffraction study of antiferromagnetic Ba_2CoWO_6 and Ba_2NiWO_6. *Journal of Applied Physics*, 1967, **38(3):** 1459.

[16] RAMMEH N, EHRENBERG H, FUESS H, *et al*. Structure and magnetic properties of the double-perovskites $Ba_2(B,Re)_2O_6$ (B=Fe, Mn, Co and Ni). *Physica Status Solidi (c)*, 2006, **3(9):** 3225.

[17] XIAO G L, LIU Q A, ZHAO F, *et al*. $Sr_2Fe_{1.5}Mo_{0.5}O_6$ as cathodes for intermediate-temperature solid oxide fuel cells with $La_{0.8}Sr_{0.2}Ga_{0.87}Mg_{0.13}O_3$ electrolyte. *Journal of Electrochem Society*, 2011, **158:** B455.

[18] MENG J L, LIU X J, HAN L, *et al*. Improved electrochemical performance

by doping cathode materials $Sr_2Fe_{1.5}Mo_{0.5-x}Ta_xO_{6-\delta}$ ($0\leqslant x\leqslant 0.15$) for solid state fuel cell. *Journal of Power Sources*, 2014, **247:** 845.
[19] DENG Z Q, SMIT J P, NIU H J, *et al*. B cation ordered double perovskite $Ba_2CoMo_{0.5}Nb_{0.5}O_{6-\delta}$ as a potential SOFC cathode. *Chemistry of Materials*, 2009, **21(21):** 5154.
[20] PRADHEESH R, NAIR H S, KUMAR C M N, *et al*. Observation of spin glass state in weakly ferromagnetic Sr_2FeCoO_6 double perovskite. *Journal of Applied Physics*, 2012, **111(5):** 053905.
[21] PRADHEESH R, NAIR HS, SANKARANARAYANAN V, *et al*. Large magnetoresistance and Jahn-Teller effect in Sr_2FeCoO_6. *The European Physical Journal B*, 2012, **85:** 260.
[22] PRADHEESH R, NAIR HS, SANKARANARAYANAN V, *et al*. Exchange bias and memory effect in double perovskite Sr_2FeCoO_6. *Applied Physics Letters*, 2012, **101(14):** 142401.
[23] CONG LG, HE TM, JI YA, *et al*. Synthesis and characterization of IT-electrolyte with perovskite structure $La_{0.8}Sr_{0.2}Ga_{0.85}Mg_{0.15}O_{3-\delta}$ by glycine-nitrate combustion method. *Journal of Alloys and Compounds*. 2003, **348(1/2):** 325.
[24] WANG Y, JIN F, HAO X, *et al*. B-site-ordered Co-based double perovskites $Sr_2Co_{1-x}Nb_xFeO_{5+\delta}$ as active and stable cathodes for intermediate-temperature solid oxide fuel cells. *Journal of Alloys and Compounds*, 2020, **829:** 154470.
[25] WU H, QIAN Y, TAN W, *et al*. The theoretical search for half-metallic material: the non-stoichiometric perovskite oxide $Sr_2FeCoO_{6-\delta}$. *Applied Physics Letters*, 2011, **99(12):** 123116.
[26] SHAO Z, XIONG G, TONG J, *et al*. Ba effect in doped $Sr(Co_{0.8}Fe_{0.2})O_{3-\delta}$ on the phase structure and oxygen permeation properties of the dense ceramic membranes. *Separation and Purification Technology*, 2001, **25(1/2/3):** 419.
[27] SHAO Z, YANG W, CONG Y, *et al*. Investigation of the permeation behavior and stability of a $Ba_{0.5}Sr_{0.5}Co_{0.8}Fe_{0.2}O_{3-\delta}$ oxygen membrane. *Journal of Membrane Science*, 2000, **172(1/2):** 177.
[28] LIU X, JIN F, LIU X, *et al*. Effect of calcium doping on $Sm_{1-x}Ca_xBaCo_2O_{5+\delta}$ cathode materials for intermediate-temperature solid oxide fuel cells. *Electrochim Acta*, 2021, **390:** 138830.
[29] LING Y H, GUO T M, GUO Y Y, *et al*. New two-layer Ruddlesden-Popper cathode materials for protonic ceramics fuel cells. *Journal of Advanced Ceramics*, 2021, **10:** 1052.
[30] JIN F, LIU J, NIU B, *et al*. Evaluation and performance optimization of double-perovskite $LaSrCoTiO_{5+\delta}$ cathode for intermediate-temperature solid-oxide fuel cells. *International Journal of Hydrogen Energy*, 2016, **41(46):** 21439.
[31] GHAFFARI M, SHANNON M, HUI H, *et al*. Preparation, surface state and band structure studies of $SrTi_{(1-x)}Fe_{(x)}O_{(3-\delta)}$ (x=0–1) perovskite-type nano structure by X-ray and ultraviolet photoelectron spectroscopy. *Surface Science*, 2012, **606(5/6):** 670.
[32] PIKALOVA EY, MARAGOU VI, DEMINA AN, *et al*. The effect of co-dopant addition on the properties of $Ln_{0.2}Ce_{0.8}O_{2-\delta}$ (Ln=Gd, Sm, La) solid-state electrolyte. *Journal of Power Sources*, 2008, **181(2):** 199
[33] JIN F, LIU J, SHEN Y, *et al*. Improved electrochemical performance and thermal expansion compatibility of $LnBaCoFeO_{5+\delta}$–$Sm_{0.2}Ce_{0.8}O_{1.9}$ (LnPr and Nd) composite cathodes for IT-SOFCs. *Journal of Alloys and Compounds*, 2016, **685:** 483.
[34] LIU B, SUNARSO J, ZHANG Y, *et al*. Highly oxygen non-stoichiometric $BaSc_{0.25}Co_{0.75}O_{3-\delta}$ as a high-performance cathode for intermediate-temperature solid oxide fuel cells. *ChemElectroChem*, 2018, **5(5):** 785.
[35] BU Y F, DING D, LAI S Y, *et al*. Evaluation of $La_{0.4}Ba_{0.6}Fe_{0.8}Zn_{0.2}O_{3-\delta}$+$Sm_{0.2}Ce_{0.8}O_{1.9}$ as a potential cobalt-free composite cathode for intermediate temperature solid oxide fuel cells. *Journal of Power Sources*, 2015, **275:** 808.
[36] LI S L, ZHANG L K, XIA T, *et al*. Synergistic effect study of $EuBa_{0.98}Co_2O_{5+\delta}$-$Ce_{0.8}Sm_{0.2}O_{1.9}$ composite cathodes for intermediate-temperature solid oxide fuel cells. *Journal of Alloys and Compounds*, 2019, **771:** 513.
[37] STEELE BCH. Survey of materials selection for ceramic fuel cells II. cathodes and anodes. *Solid State Ionics*, 1996, **86:** 1223.

双钙钛矿 $Sr_2CoFeO_{5+\delta}$ 阴极材料的制备及其中温固体氧化物燃料电池性能研究

陈正鹏[1], 金芳军[2,3], 李明飞[1], 董江波[1], 许仁辞[1], 徐韩昭[4], 熊 凯[5], 饶睦敏[1], 陈创庭[1], 李晓伟[2], 凌意瀚[2]

(1. 广东能源集团科技研究院有限公司, 广州 510000; 2. 中国矿业大学 材料科学与物理学院, 徐州 221116; 3. 长春理工大学, 长春 130022; 4. 广东省能源集团有限公司, 广州 510000; 5. 广东惠州天然气发电有限公司, 惠州 516000)

摘 要: 随着操作温度降低, 中温固体氧化物燃料电池(IT-SOFCs)需要更高催化活性的阴极材料来提升电池性能。为此, 本研究采用溶胶–凝胶法合成了双钙钛矿 $Sr_2CoFeO_{5+\delta}$ (SCF)阴极材料, 并探讨了 SCF 阴极与摩尔分数 20% Sm_2O_3 掺杂的 CeO_2(SDC)进行不同比例的复合对电极性能的影响, 优化了电极的化学膨胀和面积比电阻(ASR), 进而提升了 SOFC 单电池的电化学性能。结果表明, SCF 作为 SOFC 阴极, 经 950 ℃退火 10 h 后与普通电解质具有良好的化学相容性; 其中, SCF 与 SDC 按照质量比 1∶1 复合的样品可以将纯 SCF 样品的平均热膨胀系数(TEC)从 2.44×10^{-5} K^{-1} 显著降到 15.4×10^{-5} K^{-1}。此外, SCF–xSDC(x=20, 30, 40, 50, x 为 SDC 的质量分数)复合阴极的 ASR 在 800 ℃下分别低至 0.036、0.034、0.028 和 0.092 Ω·cm^2, SCF–40SDC 在所有温度范围内都表现出更小的 ASR。复合 SDC 可以优化 SCF 的三相界面且进一步提高 SCF 阴极的催化活性, 以 0.3mm 厚 $La_{0.9}Sr_{0.1}Ga_{0.8}Mg_{0.2}O_{3-\delta}$(LSGM)为电解质的 SCF–40SDC 单电池(757 mW·cm^{-2})比 SCF 单电池(684 mW·cm^{-2})的最大功率密度更优, 且超过目前大部分的文献报道。本研究制备的 SCF−40SDC 是一种性能优异的复合阴极材料, 有望应用于中温固体氧化物燃料电池。

关 键 词: 固体氧化物燃料电池; 双钙钛矿; 阴极; $Sr_2CoFeO_{5+\delta}$; 复合电极; 电化学性能

中图分类号: O61 **文献标志码:** A **文章编号:** 1000-324X(2024)03-0337-08

Supporting information

Double Perovskite $Sr_2CoFeO_{5+\delta}$: Preparation and Performance as Cathode Material for Intermediate-temperature Solid Oxide Fuel Cells

CHEN Zhengpeng[1], JIN Fangjun[2,3], LI Mingfei[1], DONG Jiangbo[1], XU Renci[1], XU Hanzhao4, XIONG Kai[5], RAO Muming[1], CHEN Chuangting[1], Li Xiaowei[2], LING Yihan[2]

(1. Guangdong Energy Group Science and Technology Research Institute Co. Ltd, Guangzhou 510000, China; 2. School of Materials Science and Physics, China University of Mining and Technology, Xuzhou 221116, China; 3. School of Physics, Changchun University of Science and Technology, Changchun 130022, China; 4. Guangdong Energy Group Co. Ltd., Guangzhou 510000, China; 5. Guangdong Huizhou LNG Power Co. Ltd., Huizhou 516000, China)

Experimental section

Material characterization

The phase structure of the prepared cathode and its chemical compatibility with electrolytes were characterized by X-ray diffraction (XRD, Rigaku D/Max-2550) using Cu Kα radiation (λ=0.15418 nm) at room temperature with a step size of 0.02°. The oxygen temperature programmed desorption (O_2-TPD) was carried out at 30–1000 ℃ by a chemisorption analyzer (PCA-1200, Builder, China). XPS measurements were performed using a VG Scientific ESCALAB MK II X-ray photoelectron spectrometer with a monochromatized microfocused AlKα (1486.6 eV) radiation source. The thermal expansion coefficient (TEC) was measured by a dilatometer (Netzsch DIL 402C) in the temperature range of 30−1000 ℃. The electrical conductivities of the SCF sample were measured using the van der Pauw method between 300 and 850 ℃ in air. Electrochemical performance measurements were conducted with an electrochemical analyzer (CHI604D, Chenhua). Impedance spectra were recorded in a frequency range of 0.1 Hz–1×10^5 Hz under open circuit conditions, and the signal amplitude was 10 mV.

Supplementary Tables and Figures

Table S1　Atomic occupancy information (atomic parameters) of XRD refinement

Atom	Wyck.	S.O.F.	*x*/*a*	*y*/*b*	*z*/*c*	*U*/Å^2
Sr1	8c	1	0.25	0.25	0.25	0.01083(1)
Co1	4b	1	0.5	0.5	0.5	0.01311(1)
Fe1	4a	1	0	0	0	0.0115(2)
O1	24e	1	0.2496(5)	0	0	0.00995(2)

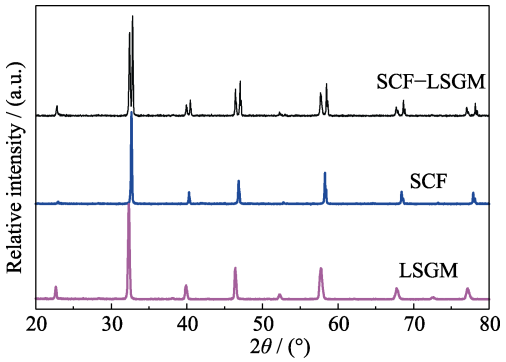

Fig. S1　XRD patterns of SCF−LSGM mixtures calcined at 950 ℃ for 10 h

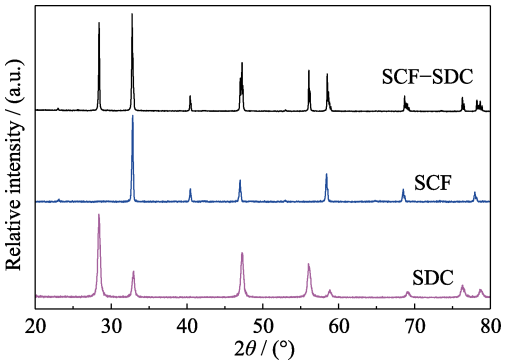

Fig. S2　XRD patterns of SCF−SDC mixtures calcined at 950 ℃ for 10 h

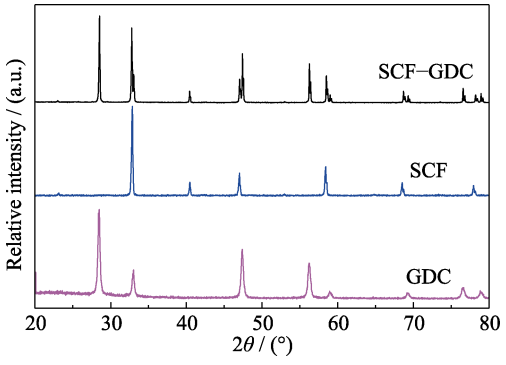

Fig. S3　XRD patterns of SCF−GDC mixtures calcined at 950 ℃ for 10 h

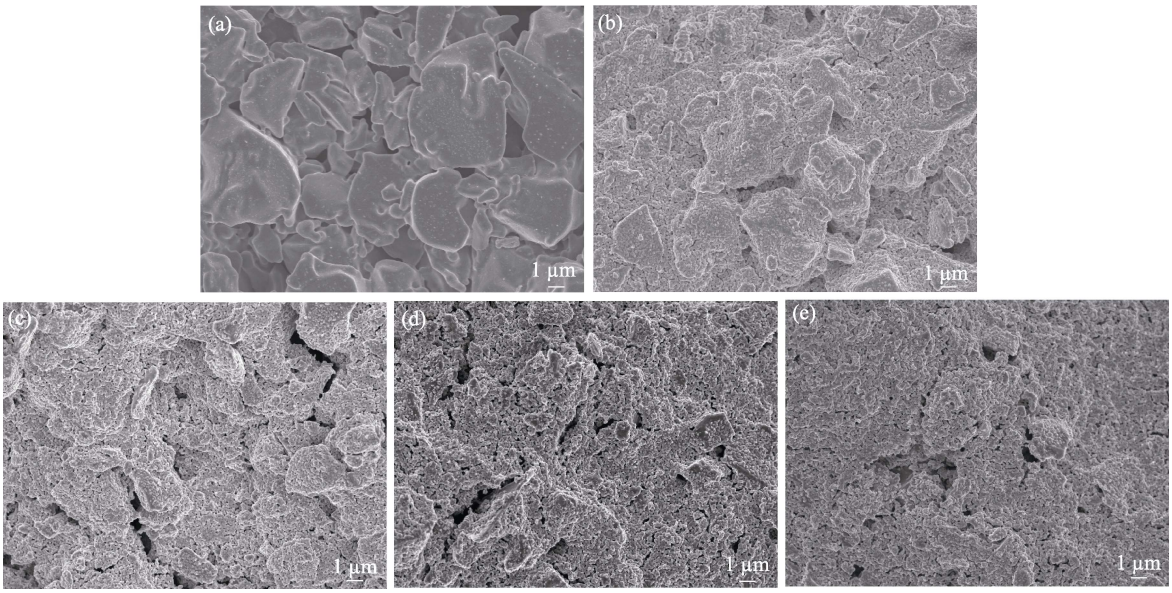

Fig. S4 SEM micrographs of (a) SCF cathode, (b) SCF−20SDC, (c) SCF−30SDC, (d) SCF−40SDC, and (e) SCF−50SDC composite cathodes

Table S2 Electrochemical performance for cathode materials using hydrogen fuels

Cathode	Electrolyte	*T*/℃	Power density/(mW·cm^{-2})	Ref.
$YBaCo_{2/3}Fe_{2/3}Cu_{2/3}O_{5+\delta}$	LSGM	800	543	[1]
$SrCo_{0.7}Fe_{0.2}Ta_{0.1}O_{3-\delta}$	LSGM	800	652.9	[2]
$PrBaCo_{2/3}Fe_{2/3}Cu_{2/3}O_{5+\delta}$	GDC	800	659	[3]
$Pr_{1.9}Ca_{0.1}BaCoFeO_{5+\delta}$	LSGM	800	728	[4]
SCF−40SDC	LSGM	800	757	This work

References:

[1] LIU J C, JIN F J, YANG X, *et al*. $YBaCo_2O_{5+\delta}$-based double-perovskite cathodes for intermediate-temperature solid oxide fuel cells with simultaneously improved structural stability and thermal expansion properties. *Electrochim Acta*, 2019, **297:** 344.

[2] QU B P, LONG W, JIN F J, *et al*. $SrCo_{0.7}Fe_{0.2}Ta_{0.1}O_{3-\delta}$ perovskite as a cathode material for intermediate-temperature solid oxide fuel cells. *International Journal of Hydrogen Energy*, 2014, **39(23):** 12074.

[3] JIN F J, SHEN Y, WANG R, *et al*. Double-perovskite $PrBaCo_{2/3}Fe_{2/3}Cu_{2/3}O_{5+\delta}$ as cathode material for intermediate-temperature solid-oxide fuel cells. *Journal of Power Sources*, 2013, **234:** 244.

[4] JIN F J, LIU X L, CHU X Y, *et al*. Effect of nonequivalent substitution of $Pr^{3+/4+}$ with Ca^{2+} in $PrBaCoFeO_{5+\delta}$ as cathodes for IT-SOFC. *Journal of Materials Science*, 2021, **56:** 1147.